Scaled Particle Theory for Wormlike Hard Spherocylinders: Calculation of Phase Diagrams for Ternary Systems Consisting of Two Semiflexible Polymers with Different Lengths and a Solvent

Takahiro Sato,* Takeshi Shoda, and Akio Teramoto

Department of Macromolecular Science, Osaka University, Toyonaka, Osaka 560, Japan

Received July 19, 1993; Revised Manuscript Received October 12, 1993®

ABSTRACT: We extended the scaled particle theory of Cotter and Wacker for multicomponent systems of straight hard spherocylinders to multicomponent solutions of wormlike hard spherocylinders and calculated phase diagrams of ternary systems consisting of two homologous semiflexible polymer components with different lengths and a low molar mass good solvent. The basic parameters in this theory are the chain contour lengths (L_1, L_2), the hard core diameter (d), and the persistence length (q) of the polymer components. The theoretical ternary phase diagrams calculated by this scaled particle theory for wormlike hard spherocylinders were compared with experimental ternary phase diagrams obtained previously for systems of schizophyllan + water and poly(n-hexyl isocyanate) + toluene. When the hard core diameter d was chosen to have a value close to that estimated from the osmotic pressure or solvent chemical potential data for the corresponding binary solutions, good agreements between experimental and theoretical ternary phase diagrams were obtained for the isotropic–anisotropic binodal curves and the tie lines of all the systems compared. On the other hand, the present theory failed to predict anisotropic–anisotropic–isotropic three-phase coexistence as well as anisotropic–anisotropic two-phase coexistence in ternary solutions containing two samples with the Kuhn segment numbers $N_1 (\equiv L_1/2q) = 0.930$ and $N_2 (\equiv L_2/2q) = 0.0765$, whereas these multiphase separations were found for aqueous solutions of schizophyllan with the same N_i's. When N_2 was decreased to smaller than 0.07 with N_1 kept at 0.93, these phase-coexisting regions appeared in the theoretical phase diagram.

Introduction

Abe and Flory[1] investigated effects of polydispersity on phase behavior in liquid crystalline polymer solutions, focusing their attention on phase diagrams for solutions containing two rodlike polymer species differing in molecular weights and a low molecular weight good solvent using the Flory lattice theory.[2,3] Features of these phase diagrams in comparison with those for monodisperse polymer solutions are summarized as follows. (1) The isotropic–anisotropic (IA) biphasic region widens by mixing two polymer species. (2) The lower molecular weight and higher molecular weight species are enriched in coexisting isotropic and anisotropic phases, respectively (the fractionation effect). (3) If the molecular weight ratio of two polymers is sufficiently large, an isotropic–anisotropic–anisotropic (IAA) triphase separation occurs. (4) There is a biphasic region for two anisotropic phases (AA) adjoining the above IAA triphase region. (Actual calculations of the AA binodals were made first by Itou and Teramoto.[4])

A few years later, all of the above characteristic features of Abe–Flory's ternary phase diagram were confirmed experimentally by Itou and Teramoto,[4,5] who studied the phase behavior in ternary aqueous solutions with two fractionated samples of a rigid triple helical polysaccharide, schizophyllan. This qualitative agreement between Abe–Flory's theoretical and the experimental phase diagrams exemplified the significance of the Flory lattice theory. However, in quantitative comparison, Itou and Teramoto found large disagreements between the theoretical and experimental phase diagrams; the Abe–Flory phase diagram exaggerates the above-mentioned characteristic features of the ternary system.

The above disagreement may be due in large part to the chain flexibility of the high molecular weight schizophyllan samples used by Itou and Teramoto; the Flory lattice theory used by Abe and Flory does not take the chain flexibility effect into account. Odijk[6] proposed to calculate ternary phase diagrams by the Onsager cluster expansion theory[7] with the following modifications. (1) A conformational entropy loss of semiflexible polymers accompanied by nematic transformation was considered by replacing the orientational entropy loss term in the free energy expression of Onsager with a conformational entropy loss term derived by Odijk himself.[6] (2) The conformational entropy loss term and the orientation-dependent intermolecular excluded volume term were calculated from a Gaussian orientational distribution function instead of the Onsager trial function. (The Gaussian distribution function makes the mathematical expressions of the two terms much simpler, although it is less accurate than the Onsager function.[6])

An actual comparison between the Odijk theory and experiment for ternary systems with two semiflexible polymer species was made by Sato et al.[8] They calculated the ternary phase diagrams for two ternary systems of aqueous schizophyllan studied by Itou and Teramoto, as well as two ternary systems of poly(n-hexyl isocyanate) (PHIC) and toluene studied by themselves. With respect to the IA binodals and the tie lines, the agreement between the theoretical and experimental phase diagrams was much improved in comparison with the Abe–Flory theory. However, the Odijk theory failed to predict the IAA triphase and the AA biphase separations for the aqueous solution containing two schizopyhllan samples with the Kuhn statistical segment numbers of 0.93 and 0.0765, which was observed experimentally and predicted successfully by Abe and Flory. In addition to this, the theoretical IA binodals obtained from the Odijk theory still slightly deviate from the experimental data toward higher polymer concentrations.

The failure of the Odijk theory may be due to the second virial approximation for the free energy as well as to the Gaussian trial function approximation for the orientational distribution function. In order to examine how these two

® Abstract published in *Advance ACS Abstracts*, December 1, 1993.

0024-9297/94/2227-0164$04.50/0

approximations affect theoretical phase diagrams, the present study calculated the ternary phase diagram for two semiflexible polymers and good solvent systems without these approximations. A scaled particle theory for multicomponent systems of wormlike hard spherocylinders was employed to remove the second virial approximation. This scaled particle theory is an extension of Cotter and Wacker's scaled particle theory[9] for multicomponent systems with different *straight* hard spherocylinder species. For the orientational distribution function, the Onsager trial function[7] was used instead of the Gaussian function.

In this paper, we describe first the extension of the Cotter–Wacker theory to multicomponent solutions containing different wormlike hard spherocylinder species. This extended scaled particle theory is used to calculate phase diagrams for ternary solutions of bidisperse wormlike chains, and the results are compared with the previous experimental results.[8]

Theory

1. Scaled Particle Theory for Multicomponent Solutions Containing Wormlike Hard Spherocylinders of Different Geometries. The scaled particle theory was originally presented by Reiss et al.[10] to calculate thermodynamic quantities of single-component hard sphere liquids. Afterward this theory was extended to monodisperse hard (sphero)cylinder systems by several authors.[11-15] Recently we[16] have extended Cotter's scaled particle theory[15] to (monodisperse) wormlike hard spherocylinder systems and obtained good agreements between theory and experiment in phase boundaries for quasi-binary solutions of several liquid crystalline polymers.

Cotter and Wacker[9] derived thermodynamic quantities for multicomponent systems consisting of straight hard spherocylinders and hard spheres using a scaled particle theory. (They considered also the van der Waals attractive interaction among constituent molecules by a mean field theory.) When the system is reduced to monodisperse hard spheres and monodisperse hard spherocylinders, their results become identical with those of Reiss et al.[10] and of Cotter,[15] respectively. The extension of the Cotter–Wacker theory to multicomponent solutions containing wormlike hard spherocylinders of different geometries can be done as follows.

Let us consider a system consisting of r components of wormlike hard spherocylinders and a (good) solvent. The geometry of a spherocylinder of species s ($s = 1, 2, ..., r$) is specified by the cylinder length L_{cs}, the hard-core diameter d_s, and the persistence length q_s; the total contour length of the spherocylinder of species s is equal to $L_{cs} + d_s$. Further, this multicomponent solution is assumed to be in dialytic equilibrium across a semipermeable membrane with the pure (single) solvent at a constant temperature T and pressure. (In this dialytic equilibrium condition, the Cotter–Wacker procedure for spherocylinder *gases* can be applied to the present wormlike spherocylinder *solutions*, as mentioned by Onsager.[7]) Under this condition, the excess Gibbs free energy ΔG of this solution over that of the solvent component is related to the reversible work W_s of adding a spherocylinder of species s to the system at an arbitrary point at a constant osmotic pressure Π by[13]

$$\frac{\Delta G}{nk_BT} = \sum_{s=1}^{r} x_s \left[\frac{\mu_s^\circ}{k_BT} + \ln(x_s c') + \sigma_{WC,s} + \frac{W_s}{k_BT} \right] \quad (1)$$

where n is the total number of spherocylinder species in the system, k_B the Boltzmann constant, x_s and μ_s° the mole fraction and the standard chemical potential of species s, respectively, and c' the total number concentration of the spherocylinder species. As mentioned by Khokhlov and Semenov,[17,18] the formation of a liquid crystal (nematic) phase in semiflexible polymer solutions is accompanied by conformational entropy loss as well as orientational entropy loss, and then the quantity $\sigma_{WC,s}$ in eq 1 times nk_B represents both entropy losses at the formation of the liquid crystal phase. An explicit expression of $\sigma_{WC,s}$ will be described in the next subsection.

In general, W_s can be related to the probability $P_s(\mathbf{a};l)$ that a wormlike spherocylinder of species s with the tangent vector $\mathbf{a}$ to the cylinder axis at the contour point l ($0 \le l \le L_{cs}$) may be inserted at some arbitrary point of the solution without overlapping any other spherocylinders existing in the solution by the equation

$$W_s = \frac{k_BT}{L_{cs}} \int_0^{L_{cs}} dl \int d\mathbf{a}\, f_s(\mathbf{a};l) \ln P_s(\mathbf{a};l) \quad (2)$$

Here, $f_s(\mathbf{a};l)$ is the orientational distribution function of the tangent vector at the contour point l. Therefore we can formulate ΔG and other thermodynamic quantities from W_s or $P_s(\mathbf{a};l)$.

However, it is somewhat involved to formulate W_s or $P_s(\mathbf{a};l)$ for the real system directly. A recipe of the scaled particle theory for this difficulty is to calculate W_s and $P_s(\mathbf{a};l)$ for a *hypothetical* scaled particle with a cylinder length λL_{cs} and a hard core diameter κd_s, and then to interpolate them to $\lambda = \kappa = 1$. For the wormlike spherocylinder, we must specify also the persistence length of the scaled particle; but it can be rather arbitrarily chosen: the only necessary condition is that it must be equal to q_s at $\lambda = \kappa = 1$. Here we assume that the persistence length of the scaled particle is just the same as that of the real wormlike spherocylinder.

When λ and κ take sufficiently small values at constant q_s, the scaled particle tends to a straight spherocylinder, and also it seldom overlaps simultaneously with two or more other spherocylinder particles at the insertion into the solution. Taking advantage of these facts, we can formulate $P_s(\mathbf{a};l)$ using the mutual excluded volume of the scaled particle and a real particle of species t with the tangent vector $\mathbf{a}'$ at the contour point l' as

$$P_s(\mathbf{a};l) = 1 - c' \sum_{t=1}^{r} x_t \Big[\lambda L_{cs}(\kappa d_s + d_t) \int_0^{L_{ct}} dl' \int d\mathbf{a}' \, |\sin\gamma(\mathbf{a},\mathbf{a}')| f_t(\mathbf{a}';l') + \frac{\pi}{4}(\kappa d_s + d_t)^2 (\lambda L_{cs} + L_{ct}) + \frac{\pi}{6}(\kappa d_s + d_t)^3 \Big] \qquad (\lambda, \kappa \ll 1) \quad (3)$$

where $\gamma(\mathbf{a},\mathbf{a}')$ is the angle between $\mathbf{a}$ and $\mathbf{a}'$.

On the other hand, when λ and κ are much larger than unity, the scaled particle becomes much greater than the other particles in the solution, so that the latter can be regarded as a continuum medium. In this case, W_s is equal to the mechanical work necessary to produce a void with the same size as the scaled particle against the osmotic pressure Π of the system. Therefore, we have

$$W_s = \Pi \Big[\frac{\pi}{4} \lambda L_{cs} (\kappa d_s)^2 + \frac{\pi}{6} (\kappa d_s)^3 \Big] \qquad (\lambda, \kappa \ll 1) \quad (4)$$

The accuracy of the scaled particle theory is determined by the interpolation method. According to Cotter and

Table 1. Parameters Appearing in the Scaled Particle Theory

parameter	heterogeneous mixture	homologous mixture
b_{st}	$\frac{\pi}{8}L_{cs}L_{ct}(d_s + d_t)$	$\frac{\pi}{4}L_{cs}L_{ct}d$
b_{st}°	$\frac{\pi}{4}[d_s^2(L_{ct} + 2d_t) + d_t^2(L_{cs} + 2d_s) + 2d_sd_t(L_{cs} + L_{ct})]$	$3(v_s + v_t)^a$
c_{stu}	$\frac{\pi^2}{8}d_sd_td_u(L_{cu} + d_u)L_{cs}L_{ct}$	$2v_u'b_{st}^a$
c_{stu}°	$\frac{\pi^2}{8}d_sd_td_u(L_{cu} + d_{cu})(L_{cs}d_t + L_{ct}d_s + d_sd_t)$	$2v_u'(v_s'' + v_t'')^a$

^{a} $v_s \equiv \frac{\pi}{4}(L_{cs}d^2 + {}^2/_3d^3)$, $v_s' \equiv v_s + \frac{\pi}{12}d^3$, $v_s'' \equiv v_s - \frac{\pi}{24}d^3$.

Wacker,[9] we use the following interpolation formula

$$W_s = C_{00} + C_{10}\lambda + C_{01}\kappa + C_{11}\lambda\kappa + C_{02}\kappa^2 + \Pi\left[\left(\frac{\pi}{4}L_{cs}d_s^2\right)\lambda\kappa^2 + \left(\frac{\pi}{6}d_s^3\right)\kappa^3\right] \quad (5)$$

The coefficients C_{ij} are determined so that eq 5 reduces to eq 2 with eq 3 at λ and $\kappa \ll 1$; eq 5 reduces to eq 4 at λ and $\kappa \gg 1$. Inputting $\lambda = \kappa = 1$ into this interpolation forumula, we obtain W_s for the corresponding real system. From this W_s and eq 1 along with some thermodynamic relations, we can derive ΔG, the excess Helmholtz free energy ΔF, the osmotic pressure Π, and the chemical potential μ_s of species s of the multicomponent solution.

The final expressions of these thermodynamic quantities are given by

$$\frac{\Delta F}{nk_BT} = \sum_{s=1}^{r} x_s\left[\frac{\mu_s^\circ}{k_BT} + (\ln x_s + \sigma_{WC,s})\right] - 1 + \ln\left(\frac{c'}{1 - \bar{v}c'}\right) + \frac{Bc'}{2(1 - \bar{v}c')} + \frac{Cc'^2}{3(1 - \bar{v}c')^2} \quad (6)$$

$$\frac{\Pi}{k_BT} = \frac{c'}{1 - \bar{v}c'} + \frac{Bc'^2}{(1 - \bar{v}c')^2} + \frac{2Cc'^3}{3(1 - \bar{v}c')^3} \quad (7)$$

$$\frac{\mu_s}{k_BT} = \ln\left(\frac{x_sc'}{1 - \bar{v}c'}\right) + \frac{B_s'c'}{2(1 - \bar{v}c')} + \frac{C_s'c'^2}{3(1 - \bar{v}c')^2} + \frac{v_s\Pi}{k_BT} + \sigma_{WC,s} \quad (8)$$

where v_s is the molecular volume of species of species s given by

$$v_s = \frac{\pi}{4}L_{cs}d_s^2 + \frac{\pi}{6}d_s^3 \quad (9)$$

and $\bar{v}$ is its number average, namely, $\bar{v} = \sum x_sv_s$; $\bar{v}c'$ is the total polymer volume fraction in the phase. The coefficients in eqs 6–8 are given by

$$B \equiv \sum_{s,t=1}^{r} x_sx_t(b_{st}^\circ + 2b_{st}\rho_{st}), \quad C \equiv \sum_{s,t,u=1}^{r} x_sx_tx_u(c_{stu}^\circ + c_{stu}\rho_{st})$$

$$B_s = \sum_{t=1}^{r} x_t(b_{st}^\circ + 2b_{st}\rho_{st})$$

$$C_s = {}^1/_3\sum_{t,u=1}^{r} x_tx_u[(c_{stu}^\circ + c_{tus}^\circ + c_{ust}^\circ) + (c_{stu}\rho_{st} + c_{tus}\rho_{tu} + c_{ust}\rho_{us})] \quad (10)$$

where the parameters b_{st}°, b_{st}, c_{stu}°, and c_{stu} are given in Table 1 for the cases of heterogeneous polymer mixtures (with different diameters and persistence lengths) and homologous polymer mixtures (with the same diameters and persistence lengths). The parameter ρ_{st} is defined by

$$\rho_{st} \equiv \frac{4}{\pi}\int\int|\sin\gamma(\mathbf{a},\mathbf{a}')|\bar{f}_s(\mathbf{a})\,\bar{f}_t(\mathbf{a}')\,d\mathbf{a}\,d\mathbf{a}' \quad (11)$$

Here we approximated the orientational distribution function $f(\mathbf{a};l)$ by the average distribution function $\bar{f}(\mathbf{a})$ along the polymer contour.

Except for the $\sigma_{WC,s}$ terms, eqs 6–8 for the wormlike hard spherocylinder system are just the same as the corresponding thermodynamic quantities for the straight hard spherocylinder system[9] with the same cylinder contour lengths, because eqs 3 and 4 and the interpolation formula (eq 5) do not contain the polymer flexibility parameter explicitly. However, if the persistence length q_s is not so large in comparison with d_s, multiple contacts between pairs of different chains should occur, and the contacts must alter thermodynamic properties of the solution, e.g., the second virial coefficient.[19] Since the present interpolation formula (eq 5) does not take into account this flexibility effect, eqs 6–8 should be applied only to semiflexible polymers whose q_s is much larger than d_s.

2. Orientational and Conformational Entropy Loss Term. When a semiflexible polymer solution transforms from an isotropic state into a nematic state, the tangent vectors to the polymer chain axis at all contour points orient more or less to the nematic director and the polymer takes an extended conformation. Therefore the polymer loses some conformational entropy in addition to the orientational entropy in the nematic state. Khokhlov and Semenov[17,18] applied Lifshitz's theory[20,21] to formulate this conformational and orientational entropy loss of semiflexible polymers using the wormlike chain model and assuming the average orientational distribution function of the tangent vector along the chain contour to be described by the Onsager trial function.[7]

They obtained explicit entropy loss expressions for the cases in which the number N of Kuhn statistical segments of the wormlike chain is much larger than unity and much smaller than unity. Replacing the orientational entropy loss term in the Onsager theory[7] by their entropy loss expression, they calculated the isotropic–nematic phase boundary concentrations for binary solutions of monodisperse semiflexible polymers with $N \ll 1$ and $N \gg 1$. The phase boundary concentrations for intermediate N were obtained using a fractional interpolation formula. However, this interpolation formula for the phase boundary concentrations is not useful for multicomponent solutions of semiflexible polymers with intermediate values of N.

Odijk[6] derived an equation for this entropy loss as a function of N using a different method from Khokhlov and Semenov, as well as using a Gaussian trial function for the orientational distribution function. Although his entropy loss equation is applicable to any N, it is not reduced to the Khokhlov–Semenov result in the limits $N \ll 1$ and $N \gg 1$ due to the Gaussian orientation distribution function he used; the Gaussian distribution function is less accurate than the Onsager. Recently DuPré and Yang[22] slightly modified Odijk's result and obtained an analytical expression for the entropy loss which empirically interpolated Khokhlov and Semenov's results. Their expres-

sion is written as

$$\sigma_{WC,s} = \ln \alpha_s - 1 + \pi e^{-\alpha_s} + {}^1/_3 N_s(\alpha_s - 1) + {}^5/_{12} \ln[\cosh({}^2/_5 N_s(\alpha_s - 1))] \quad (12)$$

where α_s and N_s are the orientation parameter included in the Onsager trial function and the Kuhn segment number of species s, respectively. In the following calculation, we use this expression for $\sigma_{WC,s}$. (Hentschke[23] proposed a different interpolation formula for $\sigma_{WC,s}$, which yields almost identical results as eq 12.)

3. Calculation of Ternary Phase Diagrams. When the solution contains two homologous polymer components, the coefficients in eqs 6–8 can be written as

$$B = 6\bar{v} + 2b_1\bar{\rho}, \quad C = 2\bar{v}'(2\bar{v}'' + b_1\bar{\rho})$$
$$B_s = 6(\bar{v} + v_s) + 4b_s\bar{\rho}_s, \quad C_s = v_s'(2\bar{v}'' + b_1\bar{\rho}) + 2\bar{v}'(\bar{v}'' + v_s'' + b_s\bar{\rho}_s) \quad (13)$$

where b_s is the cylinder-part excluded volume of the spherocylinder species s given by

$$b_s = (\pi/4)L_{cs}{}^2 d \quad (14)$$

and the bar symbols attached to v, v', and v'' mean their number averages; $\bar{\rho}$ represents the (average) reduction of the mututal excluded volume due to orientation given by

$$\bar{\rho} = x_1{}^2\rho_{11} + 2x_1x_2p_c\rho_{12} + x_2{}^2p_c{}^2\rho_{22} \quad (15)$$

and $\bar{\rho}_s$ is defined by

$$\bar{\rho}_1 = x_1\rho_{11} + x_2p_c\rho_{12}, \quad \bar{\rho}_2 = x_1\rho_{12} + 2x_2p_c\rho_{22} \quad (16)$$

Here $p_c \equiv L_{c2}/L_{c1}$.

If the Onsager trial function is used for the average orientational distribution function, ρ_{st} given by eq 11 is written as[7]

$$\rho_{ss} = \frac{4}{(\pi\alpha_s)^{1/2}}\left[1 - \frac{30}{32\alpha_s} + \frac{210}{(32\alpha_s)^2} + O(\alpha_s^{-3})\right] \quad (s = 1, 2)$$

$$\rho_{12} = \frac{4}{(2\pi)^{1/2}}\left(\frac{1}{\alpha_1} + \frac{1}{\alpha_2}\right)^{1/2}\left\{1 - \frac{3}{8}\left(\frac{1}{\alpha_1} + \frac{1}{\alpha_2} + \frac{1}{\alpha_1 + \alpha_2}\right) + \frac{15}{128}\left[\frac{8}{\alpha_1\alpha_2} - \left(\frac{1}{\alpha_1} + \frac{1}{\alpha_2} + \frac{1}{\alpha_1 + \alpha_2}\right)^2\right] + O(\alpha^{-3})\right\} \quad (17)$$

It should be noticed that eq 17 for ρ_{st} consists of asymptotic expansions with respect to α_s and α_t and then applicable only to sufficiently large α_s and α_t. In the isotropic state, all ρ_{st} are unity, so that $\bar{\rho}$ and $\bar{\rho}_s$ are given by

$$\bar{\rho} = (x_1 + p_cx_2)^2, \quad \bar{\rho}_1 = \bar{\rho}_2 = x_1 + p_cx_2 \quad (18)$$

The isotropic–anisotropic (nematic) two-phase equilibrium in the ternary system can be specified by the six state variables, c_I', c_A', x_{2I}, x_{2A}, α_1, and α_2. In what follows, the subscript I (A) represents the quantity for the isotropic phase (the anisotropic phase). When the value of x_{2I} is arbitrarily chosen between 0 and 1, the other five state variables are determined from the two stability conditions of the nematic phase

$$\partial\Delta F_A/\partial\alpha_1 = 0 \quad (19)$$

$$\partial\Delta F_A/\partial\alpha_2 = 0 \quad (20)$$

and the three phase coexistence equations

$$\Pi_I = \Pi_A, \quad \mu_{1I} = \mu_{1A}, \quad \mu_{2I} = \mu_{2A} \quad (21)$$

Since eq 19 is a quadratic equation with respect to v_Ac_A', it can be solved to give

$$v_Ac_A' = \frac{r_1 - 2r_3 - (r_1{}^2 - 4r_2r_3)^{1/2}}{2(r_1 - r_2 - r_3)} \quad (22)$$

where

$$r_1 \equiv b_1/v_A, \quad r_2 \equiv {}^2/_3 b_1v_A'/v_A{}^2,$$
$$r_3 \equiv \frac{\partial\rho_{11}/\partial\alpha_1}{x_{1A}(\partial\rho_{11}/\partial\alpha_1) + 2x_{2A}p_c(\partial\rho_{12}/\partial\alpha_1)}$$

Therefore numerical calculations are made to seek the four unknown variables c_I', x_{2A}, α_1, and α_2 to satisfy the four equations, eqs 20 and 21, using eq 22.[24]

For the convenience of comparison between theoretical and experimental phase diagrams, we represent the composition of the ternary solution by the total polymer mass concentration c_v and the weight fraction ξ_v of the polymer component 2 in the total polymers 1 and 2 in the phase v (=I and A) instead of c_v' and x_{2v}, in what follows. Further, we assign the longer polymer species as the component 1, so that p_c (=L_{c2}/L_{c1}) is smaller than unity.

When ξ_I is very close to unity on the condition that N_2 is much smaller than unity and N_1 is much larger than N_2, the above numerical analysis provided two or three solutions of (c_I, c_A, ξ_A, α_1, α_2) for one given ξ_I. Figure 1 shows the solutions of c_I, c_A, and ξ_A as functions of $1 - \xi_I$ in a range of ξ_I very close to unity for the ternary system with $L_{c1} + d = 372$ nm, $L_{c2} + d = 20$ nm, $d = 1.52$ nm, $N_1 = 0.93$, and $N_2 = 0.05$. There are two or three sets of solutions (c_I, c_A, ξ_A) for one value of ξ_I in the range of 1

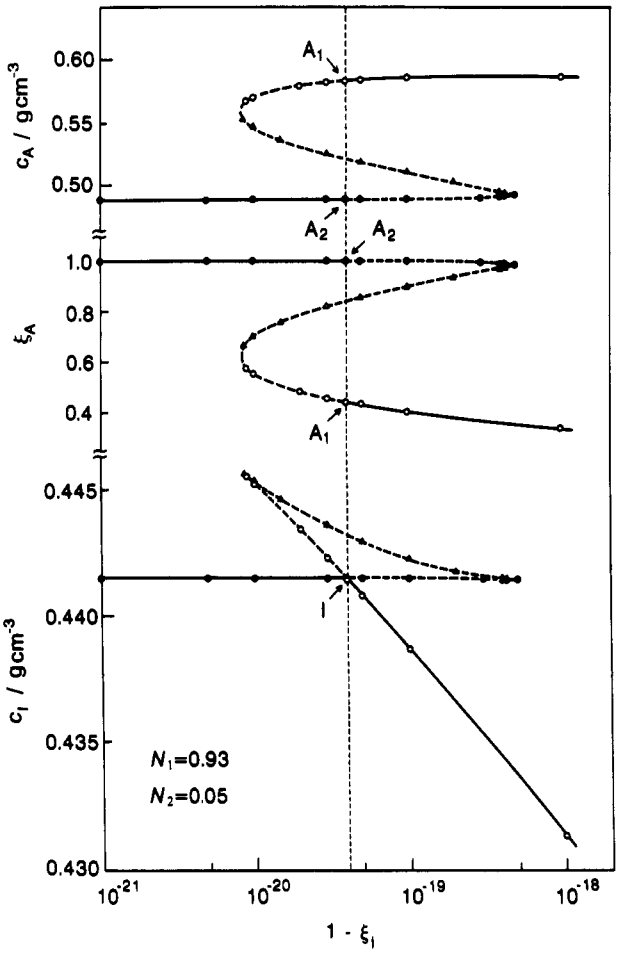

Figure 1. Multiple solutions of c_I, c_A, and ξ_A for the isotropic–nematic two-phase coexistence equations, eqs 19–21, for the system containing two wormlike hard spherocylinder species with $N_1 = 0.93$, $N_2 = 0.05$, $q = 200$ nm, and $d = 1.52$ nm; solid curves, stable solutions; broken curves, meta stable solutions.

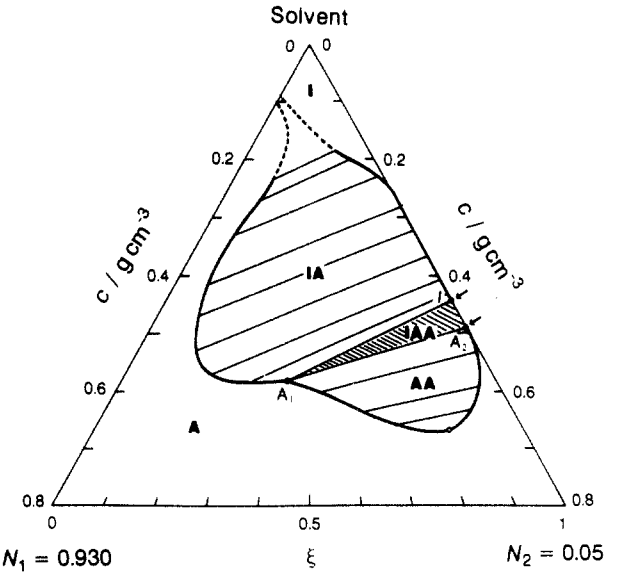

Figure 2. Ternary phase diagram for the same system as in Figure 1, possessing the isotropic (I), isotropic–nematic (IA), isotropic–nematic–nematic (IAA), nematic–nematic (AA), and nematic (A) regions; thin segments, tie lines; small circle on the AA binodal, the critical point; arrows, IA phase boundary concentrations for the binary solution with species 2.

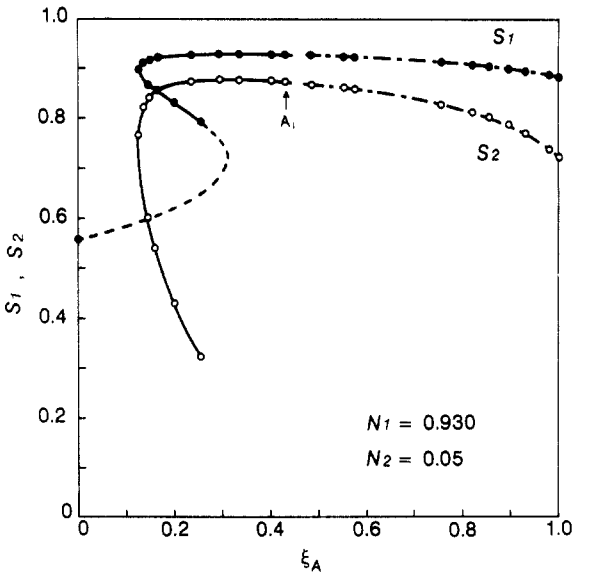

Figure 3. Orientational order parameters S_s of each component ($s = 1, 2$) for the same system as in Figure 1. The order parameter is calculated from the equation $S_s = 1 - (3/\alpha_s)\coth\alpha_s + (3/\alpha_s^2)$. The dot–dash curves correspond to the metastable nematic state between A_1 and A_2 in Figure 1.

$-\xi_I$ between 8×10^{-21} and 4×10^{-19}. (The same symbols on the three curves for c_I, c_A, and ξ_A specify one solution set.)

In Figure 1, the isotropic phase specified by point I can coexist with the two anisotropic phases indicated by points A_1 and A_2. As pointed out by Abe and Flory[1], in such a case the IAA three-phase separation occurs and only the solutions on the solid curves in Figure 1 are stable solutions for the IA biphasic equilibrium. The solutions on the broken curves in Figure 1 stand for metastable states, and the corresponding IA phase equilibria are not realized actually. It is noted that the isotropic phase as well as one anisotropic phase at the IAA phase separation is almost devoid of the longer species 1. Similar results were obtained by Abe and Flory,[1] who calculated ternary phase diagrams for rodlike polymer solutions using the Flory lattice theory.[2,3]

Coexistence of two anisotropic phases (A_1 and A_2) is expected in the vicinity of the IAA triphase region. Itou and Teramoto[4] calculated the anisotropic–anisotropic (AA) phase boundaries using the Flory lattice theory. A similar calculation can be done from our scaled particle theory by solving the following equations:

$$\partial\Delta F_{A_1}/\partial\alpha_{1A_1} = 0, \quad \partial\Delta F_{A_2}/\partial\alpha_{1A_2} = 0 \tag{23}$$

$$\partial\Delta F_{A_1}/\partial\alpha_{2A_1} = 0, \quad \partial\Delta F_{A_2}/\partial\alpha_{2A_2} = 0 \tag{24}$$

$$\Pi_{A_1} = \Pi_{A_2}, \quad \mu_{1A_1} = \mu_{1A_2}, \quad \mu_{2A_1} = \mu_{2A_2} \tag{25}$$

In a manner similar to the solution of eq 19, eq 23 can be solved for $v_{A_1}c_{A_1}$ and $v_{A_2}c_{A_2}$. Therefore, when an appropriate value of ξ_{A_1} is chosen, numerical calculations should be made to seek solutions of (ξ_{A_2}, α_{1A_1}, α_{2A_1}, α_{1A_2}, α_{2A_2}) which satisfy the above five simultaneous equations, eqs 24 and 25.

The ternary phase diagram corresponding to Figure 1 is illustrated in Figure 2. There are five regions in this theoretical phase diagram: the isotropic monophase (I), isotropic–anisotropic biphase (IA), isotropic–anisotropic–anisotropic triphase (IAA), anisotropic–anisotropic biphase (AA), and anisotropic monophase (A) regions. The thin segments in the IA and AA regions are the tie lines, and the small circle on the AA binodal curve represents a critical point. The IAA triphase region indicated by the hatched triangle was determined from the result of Figure 1.

In the small ξ region in Figure 2, c_A for the ternary solution becomes considerably lower than c_A for the binary solution of the shorter species 2 indicated by arrows. At such a low c_A, the degree of orientation parameter α_2 or the orientational order parameter S_2 of species 2 takes a very low value (cf. Figure 3), and the small values of α_2 make the asymptotic expansions of ρ_{22} and ρ_{12} given eq 17 (and also of $\sigma_{WC,2}$ given by eq 12) less accurate. Owing to these poor approximations of the orientation dependent parameters, eqs 20 and 21 become inconsistent (yielding no solutions) in the small ξ region which is indicated by the broken binodal curves in Figure 2.[25] These broken curves are the interpolation connecting c_I (and c_A) at $\xi = 0$ with that at the minimum ξ where eqs 20 and 21 have been solved.

From the theoretical binodal curves in Figure 2, we anticipate a reentrance phase behavior; i.e., when ξ of the polymer mixture is fixed at some small value (say 0.2) and the total polymer concentration c increases, the solution passes through the I monophasic, IA biphasic, A monophasic, IA biphasic, and A monophasic regions. The occurrence of similar phenomena in rodlike polymer solutions with two different length species was found by Odijk and Lekkerkerker.[26]

Comparison with Experiment

The present section compares the experimental phase diagrams for ternary systems of schizophyllan–water[4,5] and poly(n-hexyl isocyanate)–toluene[8] (PHIC–toluene) with the theoretical phase diagrams calculated from the above scaled particle theory. Equations 19–21 used for the phase diagram calculation contain five molecular parameters, L_{c1}, L_{c2}, N_1, N_2, and d. These parameters except d are calculated from the sample molecular weights along with the molar mass per unit contour length M_L and the persistence length q. The value of M_L and q for schizophyllan in water and PHIC in toluene were determined from hydrodynamic studies on their dilute solutions; the

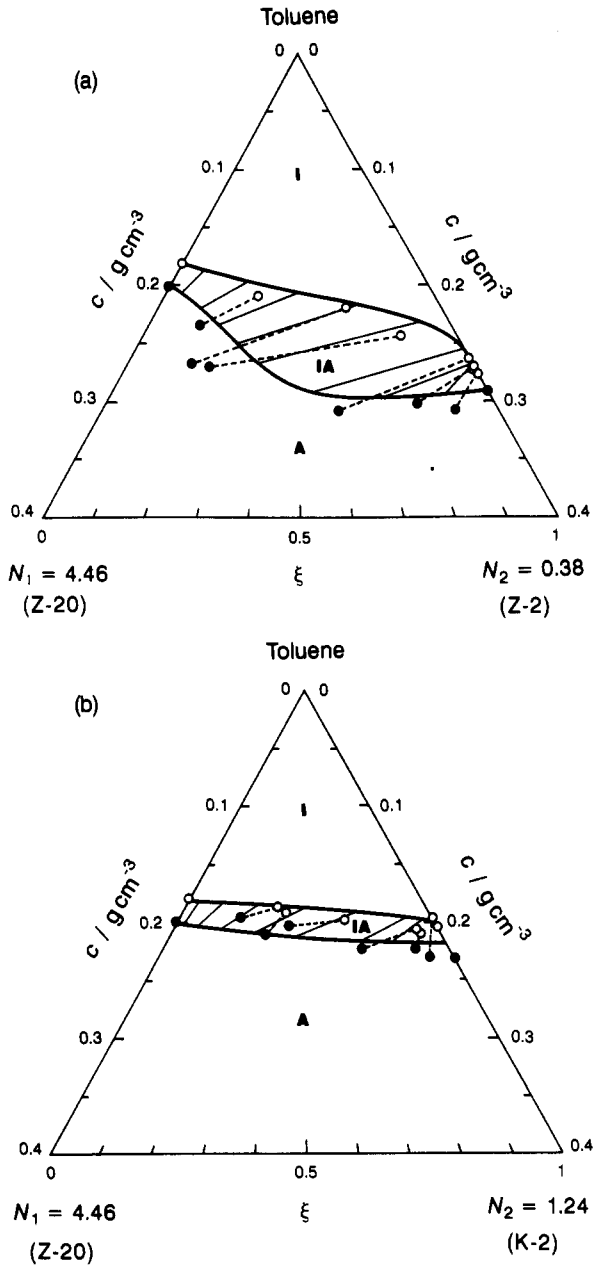

Figure 4. Comparison between the theoretical and experimental ternary phase diagrams for two toluene solutions of poly(*n*-hexyl isocyanate); solid curves and thin segments, theoretical IA binodal and tie lines obtained from the present scaled particle theory using d = 1.05 nm; circles and dotted segments, experimental IA binodal points and tie lines at 25 °C obtained by Sato et al.[8]

Table 2. Molecular Characteristics of Stiff Polymer Samples Used in Previous Ternary Phase Diagram Studies

sample	$M_w/10^4$	N	$(L_c + d)$/nm
	Poly(*n*-hexyl isocyanate)[8]		
Z-2	2.09	0.382	28.2
K-2	6.80	1.24	91.9
Z-20	24.4	4.46	330
	Schizophyllan[4,5]		
U-110	6.58	0.0765	30.6
UR-28	13.2	0.153	61.4
T-3	80.0	0.930	372

results are M_L = 2150 nm^{-1} and q = 200 nm for schizophyllan in 25 °C water[27] and M_L = 740 nm^{-1} and q = 37 nm for PHIC in 25 °C toluene.[28] The molecular parameters of the samples used in the previous phase equilibrium experiments are listed in Table 2.

Figure 4 shows theoretical phase diagrams corresponding to two ternary systems of PHIC and toluene using the

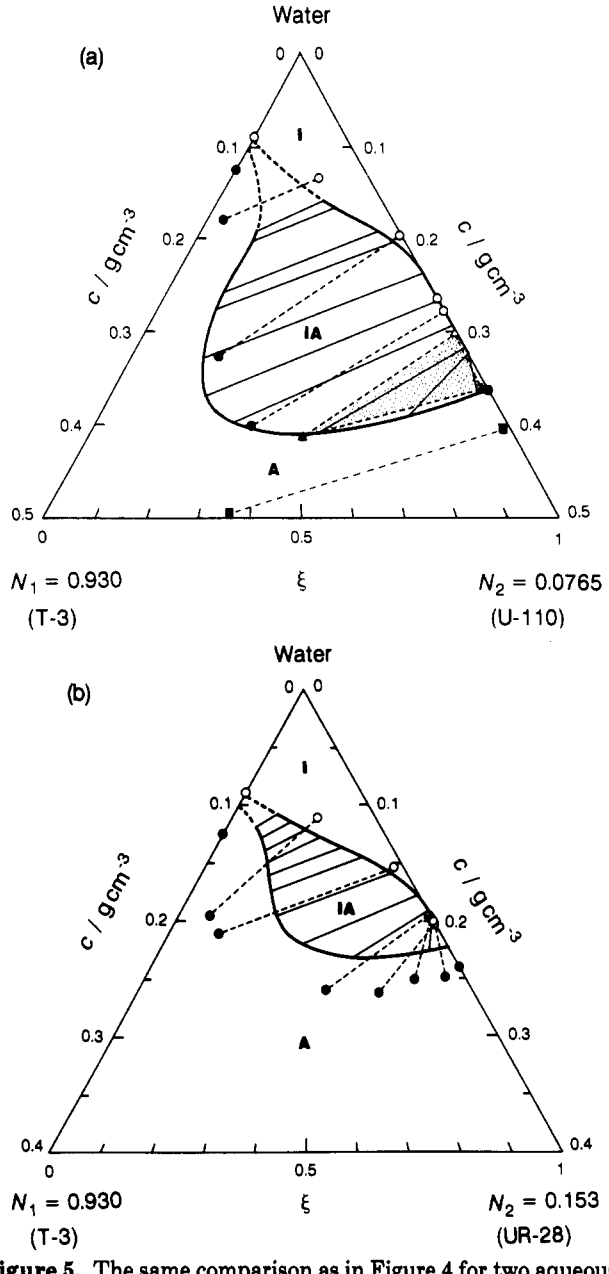

Figure 5. The same comparison as in Figure 4 for two aqueous solutions of schizophyllan at 25 °C, solid curves and thin segments, the theoretical IA binodals and tie lines calculated from the present scaled particle theory with d = 1.52 nm; circles and dotted segments, experimental IA binodal points and tie lines; shadowed triangle region and squares, experimental IAA triphasic region and the AA binodal points. The experimental data were taken from Itou and Teramoto's work.[4,5]

scaled particle theory with the hard core diameter d chosen to be 1.05 nm. The position of the theoretical isotropic–nematic biphasic regions in the two ternary phase diagrams are in good agreement with the experimental results shown by circles in the figure. Further, the theoretical tie lines (solid thin lines) successfully reproduce the fractionation effect indicated by the experimental tie lines (broken lines). The value of d chosen is close to that (1.15 nm)[16] estimated previously from comparing osmotic pressure data for binary PHIC–toluene solutions with the scaled particle theory, but slightly smaller than that (1.25 nm)[8] calculated from the partial specific volume of the same system.

Similar agreements between the scaled particle theory and experiment are also obtained for two ternary systems of aqueous schizophyllan with respect to the isotropic–cholesteric (twisted nematic) phase boundaries and tie lines. In Figure 5, the theoretical phase diagrams calcu-

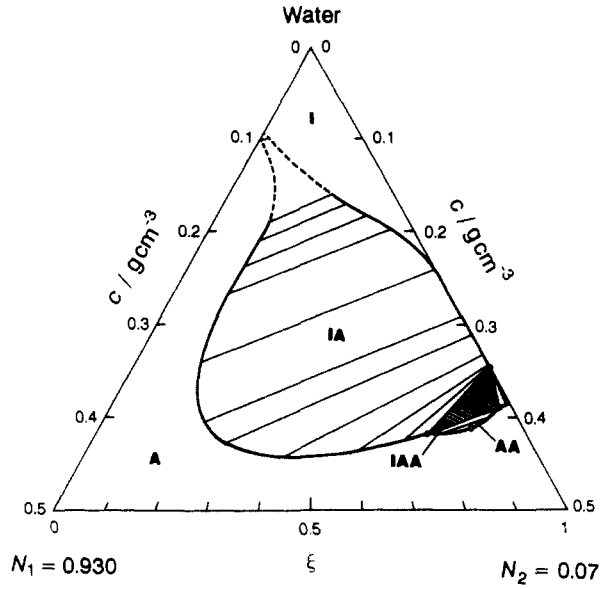

Figure 6. Theoretical ternary phase diagram corresponding to aqueous schizophyllan with $N_1 = 0.93$ and $N_2 = 0.07$; the same symbols as those in Figure 2.

lated with $d = 1.52$ nm (solid curves and thin lines) are compared with Itou and Teramoto's experimental results for aqueous schizophyllan (circles, squares, triangles, and broken lines). The value of d used is identical with that estimated previously from solvent chemical potential data for binary solutions of aqueous schizophyllan[16] but slightly smaller than that (1.67 nm) from the partial specific volume.[8] As in the case of Figure 2, there were no solutions of the IA biphasic coexistence equations, eqs 19–21, in the small ξ region of both ternary aqueous schizophyllan systems, owing to poor approximation of ρ_{st} and $\sigma_{WC,s}$ expressions (eqs 17 and 12), and the broken binodal curves are interpolation curves.

An isotropic–anisotropic–anisotropic (IAA) triphasic region and an anisotropic–anisotropic (AA) biphasic region were experimentally found only for the ternary aqueous solution of schizophyllan samples T-3 and U-110 (shadowed triangular region and squares in Figure 5a) among the four ternary solutions shown in Figures 4 and 5. The present scaled particle theory properly predicts that such multiphase regions are absent from the ternary phase diagrams for the two PHIC–toluene and one schizophyllan–water systems (Figures 4 and 5b), but it fails to predict the multiphase separations for the aqueous solution of schizophyllan T-3 and U-110. As shown previously, Odijk's theory also predicts no IAA and AA regions for the four ternary systems,[8] while Abe and Flory's theory provides the IAA and AA regions for the systems.[4] Therefore, none of the theories can correctly predict the occurrences of the IAA and AA phase separations.

If the value of N_2 (for sample U-110) is slightly reduced from 0.0765 to 0.07, the present scaled particle theory provides the IAA and AA regions in the ternary phase diagram (see Figure 6). This is in contrast with the Odijk theory, which does not predict the IAA and AA regions for any N_2 value if N_1 is fixed at 0.930. This is due to the third and higher virial terms being neglected in the Odijk theory, which must play an important role in the IAA triphase and AA biphase equilibrium occurring at rather high polymer concentrations. The Gaussian distribution function approximation is not essential to the failure of the Odijk theory to predict the IAA and AA phase separations. The scaled particle theory using the Gaussian trial function can also predict these phase separations, although the value of N_2 must be reduced below about 0.045 at N_1 fixed at 0.93.

After Itou and Teramoto's work, Kojima et al.[29] further reported the IAA and AA phase separations in aqueous solutions containing two schizophyllan samples with $N_1 = 0.930$ and $N_2 = 0.129$. This indicates that the critical value of N_2 for the onset of the IAA and AA phase separations in ternary solutions of schizophyllan with $q = 200$ nm is between 0.129 and 0.154 at N_1 fixed at 0.930. This critical value of N_2 does not agree with that predicted by the scaled particle theory (0.07). The disagreement may be ascribed to some approximations used in the present theory (e.g., eqs 5, 12, 17). However, taking into account the fact that the triphasic equilibrium must be determined by very delicate balances of the osmotic pressure and the chemical potentials of the two polymer species among the three coexisting phases, this disagreement does not indicate an essential discrepancy in ΔF between the real system and the scaled particle theory.

References and Notes

(1) Abe, A.; Flory, P. J. *Macromolecules* **1978**, *11*, 1122.
(2) Flory, P. J. *Proc. R. Soc. London* **1956**, *A234*, 73.
(3) Flory, P. J.; Abe, A. *Macromolecules* **1978**, *11*, 1119.
(4) Itou, T.; Teramoto, A. *Polym. J.* **1984**, *16*, 779.
(5) Itou, T.; Teramoto, A. *Macromolecules* **1984**, *17*, 1419.
(6) Odijk, T. *Macromolecules* **1986**, *19*, 2313.
(7) Onsager, L. *Ann. N.Y. Acad. Sci.* **1949**, *51*, 627.
(8) Sato, T.; Ikeda, N.; Itou, T.; Teramoto, A. *Polymer* **1989**, *30*, 311.
(9) Cotter, M. A.; Wacker, D. C. *Phys. Rev. A* **1978**, *18*, 2669.
(10) Reiss, H.; Frisch, H. L.; Lebowitz, J. L. *J. Chem. Phys.* **1959**, *31*, 369.
(11) Cotter, M. A.; Martire, D. E. *J. Chem. Phys.* **1970**, *53*, 4500.
(12) Cotter, M. A.; Martire, D. E. *J. Chem. Phys.* **1970**, *52*, 1909.
(13) Lasher, G. *J. Chem. Phys.* **1970**, *53*, 4141.
(14) Cotter, M. A. *Phys. Rev. A* **1974**, *10*, 625.
(15) Cotter, M. A. *J. Chem. Phys.* **1977**, *66*, 1098.
(16) Sato, T.; Teramoto, A. *Mol. Cryst. Liq. Cryst.* **1990**, *178*, 143.
(17) Khokhlov, A. R.; Semenov, A. N. *Physica* **1981**, *108A*, 546.
(18) Khokhlov, A. R.; Semenov, A. N. *Physica* **1982**, *112A*, 605.
(19) Yamakawa, H.; Stockmayer, W. H. *J. Chem. Phys.* **1972**, *57*, 2843.
(20) Lifshitz, I. M. *Soviet Phys. JETP* **1969**, *28*, 1280.
(21) Lifshitz, I. M.; Grosberg, A. Y.; Khokhlov, A. R. *Rev. Mod. Phys.* **1978**, *50*, 684.
(22) DuPré, D. B.; Yang, S. *J. Chem. Phys.* **1991**, *94*, 7466.
(23) Hentschke, R. *Macromolecules* **1990**, *23*, 1192.
(24) From eqs 19 and 20, we can also obtain an analytical equation for x_{2A}. However, this equation is a division of two very small quantities, both of which are functions of α_1 and α_2, so that it is very sensitive to small variations of the degree of orientation parameters. Therefore this equation of x_{2A} is not suitable for numerical analysis seeking the solution of three unknowns (c_I', α_1, and α_2), and we did not use this equation of x_{2A} in the actual numerical calculation of the IA binodals.
(25) In the previous ternary phase diagram calculations based on the Odijk theory, we were able to solve the phase coexistence equations, eqs 20 and 21, for any values of ξ_I. This is because c_A and then α_2 are large even at small ξ_I and ξ_A due to the second virial approximation and also the Gaussian approximation for the distribution function used in the previous calculation.
(26) Odijk, T.; Lekkerkerker, H. N. W. *J. Phys. Chem.* **1985**, *89*, 2090.
(27) Yanaki, T.; Norisuye, T.; Fujita, H. *Macromolecules* **1980**, *13*, 1462.
(28) Itou, T.; Chikiri, H.; Teramoto, A.; Aharoni, S. M. *Polym. J.* **1988**, *20*, 143.
(29) Kojima, T.; Itou, T.; Teramoto, A. *Polym. J.* **1987**, *19*, 1225.